

## Biocompatibility of cobalt iron oxide magnetic nanoparticles in male rabbits

Tanveer Ahmad Tabish<sup>\*,\*\*\*,†</sup>, Muhammad Naeem Ashiq<sup>\*\*\*,†</sup>, Muhammad Azeem Ullah<sup>\*</sup>, Shahid Iqbal<sup>\*\*\*\*</sup>,  
Muhammad Latif<sup>\*\*\*\*</sup>, Muhammad Ali<sup>\*\*\*\*\*</sup>, Muhammad Fahad Ehsan<sup>\*\*\*\*\*</sup>, and Furhan Iqbal<sup>\*\*\*\*,†</sup>

<sup>\*</sup>Institute of Advanced Materials, Bahauddin Zakariya University, Multan 60800, Pakistan

<sup>\*\*</sup>College of Engineering, Mathematics and Physical Sciences, University of Exeter, EX4 4QF United Kingdom

<sup>\*\*\*</sup>Institute of Chemical Sciences, Bahauddin Zakariya University, Multan 60800, Pakistan

<sup>\*\*\*\*</sup>Institute of Pure and Applied Biology, Zoology Division, Bahauddin Zakariya University, Multan 60800, Pakistan

<sup>\*\*\*\*\*</sup>Faculty of Veterinary Sciences, Bahauddin Zakariya University, Multan 60800, Pakistan

<sup>\*\*\*\*\*</sup>National Center for Nanoscience and Technology (NCNST), Beijing, China

(Received 2 November 2015 • accepted 9 February 2016)

**Abstract**—Present study was conducted to study the in vivo biocompatibility of cobalt iron oxide magnetic nanoparticles (CoFe<sub>2</sub>O<sub>4</sub> MNPs) in rabbits. CoFe<sub>2</sub>O<sub>4</sub> MNPs were synthesized by the conventional micro emulsion technique in crystallite size range of 30 to 50 nm. The lattice constant (a) and cell volume were found to be 8.386 Å and 589.75 Å<sup>3</sup>, respectively, revealed by XRD. Subject animals were divided in three groups—low dose, high dose and control group without nanoparticles implantation for biocompatibility evaluation. CoFe<sub>2</sub>O<sub>4</sub> was intraperitoneally implanted in rabbits: low dose (1 mg CoFe<sub>2</sub>O<sub>4</sub>/Kg body weight) and high dose (10 mg CoFe<sub>2</sub>O<sub>4</sub>/Kg body weight). Blood, serum and histological study of vital organs (liver, heart, kidney and spleen) were carried out in seven days of time protocol after sacrificing of animals. Results indicated that CoFe<sub>2</sub>O<sub>4</sub> had drastically affected the blood chemistry in a dose-dependent manner as RDW<sub>a</sub> (P<0.01), Platelet (P<0.001) and Plateletcrit (P<0.001) concentrations reduced significantly in low dose and high dose CoFe<sub>2</sub>O<sub>4</sub> treatments as compared to sham treated control group. Histological analysis revealed that CoFe<sub>2</sub>O<sub>4</sub> exposure resulted in disordered and abnormal histology of liver, kidney and that of muscles at surgical site. It is concluded that CoFe<sub>2</sub>O<sub>4</sub> has low biocompatibility and higher toxicity levels in living system at the applied doses.

**Keywords:** CoFe<sub>2</sub>O<sub>4</sub>, Micro Emulsion Synthesis, Male Rabbit, Hematology, Serum Biochemistry, Histology

### INTRODUCTION

Iron oxide nanoparticles (NPs) have extensively been studied in living systems as the carriers of therapeutic agent and in humans for clinical purposes [1]. Owing to their magnetic characteristics, small diameter, water solubility and low toxicity, these NPs are useful in life sciences such as in bio-imaging, bio-sensing and drug delivery systems [2]. NPs being used for such applications should generally offer super paramagnetism at room temperature [3]. For instance, magnetic particles, with or without immunospecific coating, are found positively responsive towards red blood cells [4,5], lung cancer cells [6] and urological cancer cells [7]. Besides iron oxide, other iron containing compounds such as spinel ferrites also have magnetic properties and can be represented by a general expression of MFe<sub>2</sub>O<sub>4</sub> (where M=Mn or Co) and more commonly synthesized by sol-gel method [8]. A number of other synthesis routes can be adopted to prepare Co ferrite particles such as chemical co-precipitation [9], combustion reaction [10,11], forced hydrolysis [12] and microemulsion approach [13]. Chemical reaction in each method proceeds at the characteristic reaction temperature, reactants addition rate and reactants concentration [14] which essen-

tially influence the size and shape of particles. Therefore, selection of a particular method is made by keeping in view the required final shape and size of nanoparticles. In the present work we have chosen the normal microemulsion method because it has many advantages other methods, such as low temperature annealing; the use of surfactant which forms the micelles that are helpful in controlling the size and shape of the particles and homogeneity can be obtained in the samples with this method. These physical parameters primarily govern the magnetic properties of ferrite spinels [15, 16]. A recent study revealed that there is no significant difference in cytotoxic behavior of Co ferrite particles when used with and without polysiloxane coating and they accumulate on intracellular sites in either case [17]. These nanoparticles retain considerable magnetization even after coating with alginate [18], which is a positive feature for their possible use in biomedical applications.

Present study discusses synthesis of cobalt ferrite nanoparticles by using normal microemulsion method and to study their biocompatibility in healthy male rabbits (*Lepus nigricollis*) by comparing the effect of low and high doses of CoFe<sub>2</sub>O<sub>4</sub> on complete blood count, selected parameters of serum biochemical profile and on the histology of selected vital organs with sham treated controls.

### MATERIALS AND METHODS

#### 1. Synthesis of CoFe<sub>2</sub>O<sub>4</sub> Nonmaterial

The chemicals used for the synthesis of cobalt ferrite nanomate-

<sup>†</sup>To whom correspondence should be addressed.

E-mail: furhan.iqbal@bzu.edu.pk

<sup>‡</sup>These authors have contributed equally to the manuscript.

Copyright by The Korean Institute of Chemical Engineers.

rials were  $\text{Co}(\text{NO}_3)_2 \cdot 6\text{H}_2\text{O}$  (Merck, >99%),  $\text{Fe}(\text{NO}_3)_3 \cdot 9\text{H}_2\text{O}$  (Riedel-de Haen, 97%), cetyltrimethyl ammonium bromide (Merck, 97%), methanol (Merck, 99%) and ammonia solution (Fisher Scientific, 35%). These chemicals were used as such without further treatment. Cobalt ferrite with composition  $\text{CoFe}_2\text{O}_4$  was synthesized by the normal microemulsion method. The required stoichiometric amount of the metal salts was dissolved in deionized water and mixed in a beaker. The cetyltrimethyl ammonium bromide (CTAB), acting as surfactant, was also added in metals solutions with ratio 1 : 1.5 (metals: CTAB). The solution was stirred on the magnetic hot plate at 60 °C until it formed a clear solution. The ammonia solution (2 M) was added dropwise to form the precipitates. The precipitates were washed several times with deionized water and finally with methanol. These precipitates were then dried at 100 °C in an oven and ground into fine powder. Finally, these were annealed at 800 °C for 8 hours in an electric furnace (Vulcan A-550). The synthesized materials were characterized by x-ray diffraction analysis by using Bruker D8 focus diffractometer with Ni-filtered  $\text{Cu-K}\alpha$  radiation to confirm the formation of cobalt ferrite. The surface morphology and particle size was determined by using scanning electron microscopy (Hitachi S4800 FE-SEM). Particle size measurements of all the samples were by HORIBA scientific nanoparticle analyzer SZ-100.

## 2. Experimental Animals

Adult male rabbits (*Lepus nigricollis*) were used as experimental animals and were maintained in cages at the animal facility, Institute of Pure and Applied Biology (IPAB), Bahauddin Zakariya University, Multan, Pakistan. Rabbits were provided with fresh vegetables and drinking water. Room temperature was maintained at  $22 \pm 1$  °C. The light/dark rhythm was maintained at 14 : 10 hours. The room was illuminated with artificial light at an intensity of about 200 W from 8 a.m. to 6 p.m. All the experimental protocols and mouse handling procedures were approved by the ethical committee of IPAB at Bahauddin Zakariya University Multan, Pakistan.

## 3. Experimental Design and Implantation of Cobalt Iron Oxide

Rabbits were acclimatized at animal facility for ten days and then divided into three groups. T1 (Sham surgery group); T2 (exposed to low dose of cobalt iron oxide) and T3 (exposed to high dose of cobalt iron oxide). Each rabbit was anesthetized using isoflurane (3%) inhalation. A left lateral incision was made in the lower abdominal region and T2 was Intraperitoneally implanted with 1 mg/Kg body weight while T3 with 10 mg/Kg body weight of cobalt iron oxide and ligated with polypropylenedalcon USP 6 suture.

## 4. Blood and Serum Collection

After seven days of surgery, rabbits were anesthetized with 3% Isoflurane and blood was sampled either from marginal ear vein. Blood was divided into two parts: one for the study of complete blood count, and the second for the determination of selected serum biochemical parameters.

Hematological parameters [Red blood cells (RBC), Hematocrit (HCT), mean corpuscular volume (MCV), hemoglobin (HGB), mean corpuscular hemoglobin (MCH), platelets (PLT), white blood cells (WBC), lymphocytes (LYM), gGranulocytes (GRANL), minimum inhibitory dilution (MID)] and serum biochemical parameters [Cholesterol, aspartate transaminase (AST), alanine transaminase (ALT), total protein and triglycerides] were determined in blood

samples from three treatments of male rabbit by using Hitachi 902 automatic analyzer (Japan).

## 5. Histology of Vital Organs

At the end of the experimental phase, the animals were sacrificed under isoflurane inhalation and heart, liver, kidney and muscles, from adjoining area where cobalt iron oxide was implanted, were surgically removed from each treatment for histopathological study. Tissues were sliced and fixed in fixative solution (containing ethanol, formaldehyde and glacial acetic acid in 60 : 30 : 10 ratio) for five hours at room temperature. Tissues were transferred to 80% ethanol over night then in 90% ethanol for two hours followed by five hours dehydration in absolute ethanol. Tissues were then transferred in clove oil and kept until they became transparent. After clearing the tissues were immersed in benzole twice for ten minutes at room temperature to remove clove oil and then were transferred in a mixture of melted paraffin and benzole (1 : 1) for 20 minutes at 60 °C and then kept in paraplast for 12 hours at 60 °C. This step was repeated thrice and each time fresh paraplast was used. The sections were cut out of paraffin block at 6  $\mu\text{m}$  by using Reichert microtome. Sections were affixed to precleaned albumenized glass slides and stretched at 60 °C on Fisher slide warmer and transferred to an incubator for complete deparaffinization at 60 °C. The slides were then put in xylene, twice for 15 minutes each, to remove the remaining paraplast. The slides were then rehydrated in descending grades of ethanol (100, 90, 70, 50 and 30% each for 2-5 minutes), washed in tap water and stained in hematoxylin, dipped in tap water for ten minutes to stain the cell nucleus with hematoxyline. Slides were dehydrated in ascending grades of ethanol (30, 50, 70 and 90% each for 2-5) and counter-stained with eosin (cytoplasm staining) by giving 2-3 dips. Slides were then dipped in 90% and absolute ethanol for 3-5 minutes for complete dehydration and cleared in xylene for ten minutes. The slides were mounted with Canada balsam. Slides were cleared, labeled, numbered and stored in slide box for microscopic observations. Photographs of selected areas in slides were taken by Nikon Optiphot (Olympus, New York) research microscope equipped with digital camera (Sony, Japan) and were compared between treated and untreated fish groups.

## 6. Statistical Analysis

All the data was expressed as Mean  $\pm$  Standard deviation. Statistical package Minitab (version 13, Pennsylvania) was used for the analysis of results. One-way ANOVA was applied to compare various parameters of hematology and serum biochemical profile of male rabbit between all three treatments.

# RESULTS

## 1. Indexed XRD Pattern for $\text{CoFe}_2\text{O}_4$ Synthesized by the Normal Microemulsion Method

It is obvious from Fig. 1 that all the peaks are perfectly matched with the standard pattern with reference code ICSD 00-001-1121, which indicates that there was no impurity in the synthesized material. The crystallite size was calculated by the well known Scherrer's formula and was found in the range of 30 to 50 nm range. The lattice constant (a) and cell volume were also calculated from XRD data and were found to be 8.386 Å and 589.75 Å<sup>3</sup>, respec-

tively, which was also in agreement with the standard values.

## 2. Scanning Electron Microscopy (SEM) and Particle Size Distribution

The SEM micrograph for the  $\text{CoFe}_2\text{O}_4$  is shown in Fig. 2. It can be observed that the particles are round and have clear boundar-

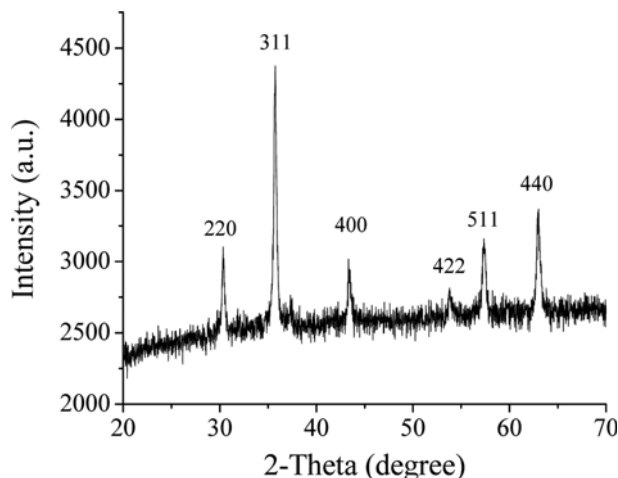


Fig. 1. Indexed XRD pattern for cobalt ferrite.

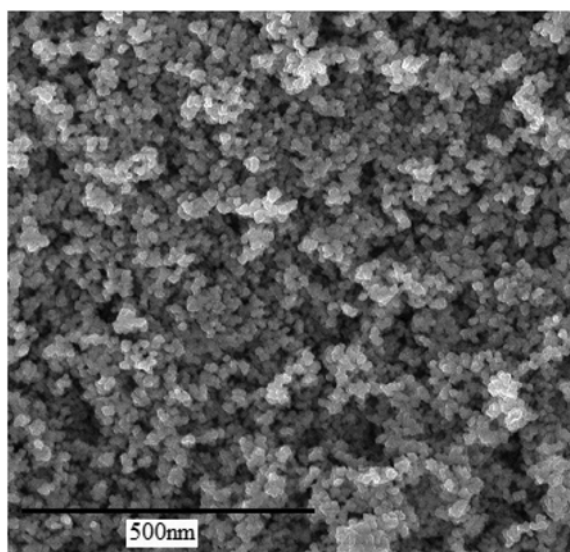


Fig. 2. SEM image for the  $\text{CoFe}_2\text{O}_4$ .

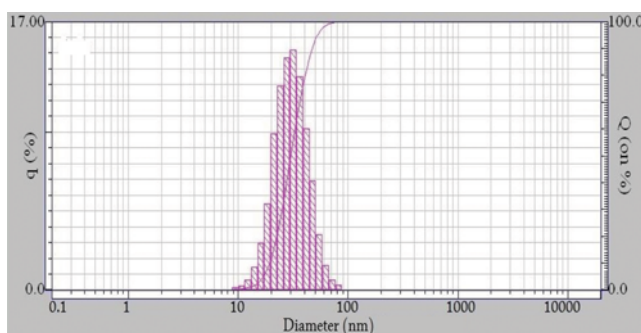


Fig. 3. Particle size distribution of cobalt ferrites.

ies. Some of the particles were agglomerated into bigger particles. The particle size calculated by scanning electron microscopy was found to be in the range of 35 to 60 nm. Fig. 3 shows the statistical distribution of the particles measured by the particle size analyzer. The average size of the particles is in agreement.

## 3. Effect of Intraperitoneal Implantation of $\text{CoFe}_2\text{O}_4$ on Complete Blood Count in *Lepus nigricollis*

Data analysis revealed a severe effect of  $\text{CoFe}_2\text{O}_4$  on complete blood count of male rabbits. It was observed that red blood cell distribution width absolute [RDWa] ( $P=0.01$ ), Platelet ( $P<0.001$ ) and Plateletcrit [PCT] ( $P<0.001$ ) concentrations decreased significantly while packed cell volume [HCT] ( $P=0.001$ ), hemoglobin [HGBL] ( $P=0.04$ ) and large platelet concentration ratio [LPCR] ( $P=0.003$ ) increased in both  $\text{CoFe}_2\text{O}_4$  treatments (T2 and T3) as compared to sham treated control group (T1). Lymphocyte [Lym] ( $P=0.03$ ) and minimum inhibitory dilution [MIDH] ( $P=0.03$ ) were affected in a dose dependent manner with more severe changes observed in T3, while all the remaining studied parameters re-

**Table 1. Comparison of complete blood count in adult male rabbit (*Lepus nigricollis*) between T1 (sham surgery), T2 (intraperitoneal implantation of 1 mg/Kg body weight of  $\text{CoFe}_2\text{O}_4$ ) and T3 (Intraperitoneal implantation of 10 mg/Kg body weight  $\text{CoFe}_2\text{O}_4$ ). All values are expressed as mean $\pm$ standard deviation. P-value indicates the probability of one way analysis of variance (ANOVA)**

Parameters	T1	T2	T3	P-value
RBC ( $\times 10^6 \mu\text{L}^{-1}$ )	4.72 $\pm$ 0.6	4.98 $\pm$ 0.6	5.78 $\pm$ 0.6	0.45
HCT (%)	28.5 $\pm$ 0.6	30.6 $\pm$ 0.6	34.5 $\pm$ 0.6	0.001***
MCV (fL)	60.4 $\pm$ 0.6	61.5 $\pm$ 0.6	59.6 $\pm$ 0.6	0.14
RDW% (H) (%)	15 $\pm$ 0.6	14.2 $\pm$ 0.6	13.5 $\pm$ 0.6	0.26
RDWa (fL)	40.9 $\pm$ 0.6	40.7 $\pm$ 0.6	37.6 $\pm$ 0.6	0.01**
HGB L (gdL $^{-1}$ )	9.4 $\pm$ 0.6	10.3 $\pm$ 0.6	12.1 $\pm$ 0.6	0.04*
MCH L (pg)	19.9 $\pm$ 0.6	20.8 $\pm$ 0.6	21 $\pm$ 0.6	0.41
MCHC (gdL $^{-1}$ )	32.9 $\pm$ 0.6	33.9 $\pm$ 0.6	35.2 $\pm$ 0.6	0.08
PLT ( $\times 10^3 \mu\text{L}^{-1}$ )	824 $\pm$ 0.6	480 $\pm$ 0.6	230 $\pm$ 0.6	$P<0.001$ ***
PCT (%)	0.44 $\pm$ 0.6	0.29 $\pm$ 0.6	0.13 $\pm$ 0.6	$P<0.001$ ***
MPV L (fL)	5.3 $\pm$ 0.6	6.1 $\pm$ 0.6	5.9 $\pm$ 0.6	0.62
PDW (fL)	8.1 $\pm$ 0.6	9.1 $\pm$ 0.6	8.9 $\pm$ 0.6	0.48
LPCR (%)	2.5 $\pm$ 0.6	6.9 $\pm$ 0.6	6.4 $\pm$ 0.6	0.003**
WBC ( $\times 10^3 \mu\text{L}^{-1}$ )	6.6 $\pm$ 0.6	11.2 $\pm$ 0.6	5.1 $\pm$ 0.6	0.001***
LYM (%)	2.1 $\pm$ 0.6	5.1 $\pm$ 0.6	3.3 $\pm$ 0.6	0.03*
GRANL (%)	1.9 $\pm$ 0.6	2 $\pm$ 0.6	0.6 $\pm$ 0.6	0.14
MID H (%)	2.6 $\pm$ 0.6	4.1 $\pm$ 0.6	1.2 $\pm$ 0.6	0.03*

Where RBC=Red blood cells, HCT=Hematocrit (pack cell volume), MCV=Mean corpuscular volume, RDW=Red blood cell distribution width, RDWa=Red blood cell distribution width (absolute), HGB=Hemoglobin, MCH=Mean corpuscular hemoglobin, PLT=Platelets, PCT=Plateletcrit, MPV=Mean platelet volume, PDW=Platelet distribution width, LPCR=large platelet concentration ratio, WBC=White blood cells, LYM=Lymphocytes, GRANL=Granulocytes, MID=Minimum inhibitory dilution,  $P>0.05$ =Non Significant;  $P<0.05$ =Least Significant (\*);  $P<0.01$  Significant (\*\*) and  $P<0.001$  Highly Significant (\*\*\*)

remained unaffected upon comparison between the three experimental treatments (Table 1).

#### 4. Effect of Intraperitoneal Implantation of $\text{CoFe}_2\text{O}_4$ on Serum Biochemical Profile in *Lepus nigricollis*

When serum biochemical parameters were compared between the experimental groups, it was observed that all the studied parameters, cholesterol, triglycerides, alanine transaminase [ALT], aspartate transaminase [AST] and total protein had higher concentrations in T2 and T3 than T1 (sham treated control), but AST ( $P=0.001$ ) was the only parameter that varied significantly among the three treatments (Table 2).

#### 5. Effect of Intraperitoneal Implantation of $\text{CoFe}_2\text{O}_4$ on the Histology of Selected Vital Organs in *Lepus nigricollis*

##### 5-1. Liver

The liver of *Lepus nigricollis* is made up of a homogeneous mass of hepatic cells containing large, round, centrally located nuclei in

cytoplasm. Normally, hepatocytes are polyhedral cells having different sizes and shapes. Channel-like sinusoids separate the hepatic tissue into lobules and cords (Fig. 4(a)). There was no major change in hepatocytes visible in T2 and T3 as the hepatocytes were of normal shape and many cells were undergoing mitosis as a divided nucleus was visible in all three treatments. In T2 and T3, cytoplasmic vacuolation and increase in sinusoidal spaces were observed, indicating minor alteration in liver histology (Fig. 4(b), (c)).

##### 5-2. Muscles from Surgery Site

Implantation of  $\text{CoFe}_2\text{O}_4$  resulted in severe histological damage to the muscle fibers at the site of implantation in T2 and T3 as myofibrils were lacking their compact smooth fiber-like pattern in all treated animals (Fig. 4(e), (f)), while normal muscle histology was visible in T1 (1D), indicating that  $\text{CoFe}_2\text{O}_4$  was responsible for this muscular atrophy.

##### 5-3. Kidney

In T1, kidney section showed normal cuboidal cell in renal tubule with prominent nucleus and eosinophilic cytoplasm. Interstitium of the tubules was infiltrated with hematopoietic tissues which contain round to polygonal cells having nuclei (Fig. 5(a)). There was marked cellular infiltration (Bold arrow), and shrinkage of tuft of capillaries in glomerulus resulted in increased urinary space (arrow head) in kidney sections of T2 and T3. Necrosis in cuboidal epithelium of renal tubules was evident, indicating severe damage to kidney histology in  $\text{CoFe}_2\text{O}_4$  exposed treatments (Fig. 5(b), (c)).

##### 5-4. Heart

Histology of the heart was intact in all three treatments. There was no sign of hemorrhages and cellular infiltration in heart parenchyma in T1, T2 and T3, indicating that  $\text{CoFe}_2\text{O}_4$  implantation did not affect the cardiac histology (Fig. 5(d)-(f)).

**Table 2.** Comparison of selected parameters of serum biochemical profile in adult male rabbits (*Lepus nigricollis*) between T1 (sham surgery), T2 (Intraperitoneal implantation of 1 mg/Kg body weight of  $\text{CoFe}_2\text{O}_4$ ) and T3 (Intraperitoneal implantation of 10 mg/Kg body weight  $\text{CoFe}_2\text{O}_4$ ). All values are expressed as mean  $\pm$  standard deviation. P-value indicates the probability of one way analysis of variance (ANOVA)

Parameters	T1	T2	T3	P-value
Cholesterol ( $\text{mgdL}^{-1}$ )	64 $\pm$ 0.6	94 $\pm$ 0.6	77.5 $\pm$ 14.2	0.1
Triglycerides ( $\text{mgdL}^{-1}$ )	57 $\pm$ 0.6	58.0 $\pm$ 0.6	93.0 $\pm$ 19.1	0.1
ALT ( $\mu\text{L}^{-1}$ )	29 $\pm$ 0.6	35.0 $\pm$ 0.6	30 $\pm$ 4.6	0.3
AST ( $\mu\text{L}^{-1}$ )	39 $\pm$ 0.6	65.0 $\pm$ 0.6	66.0 $\pm$ 4.6	0.001***
Total Protein ( $\text{gdL}^{-1}$ )	8.7 $\pm$ 0.6	9.4 $\pm$ 0.6	9.2 $\pm$ 0.2	0.6

Where ALT is Alanine Transaminase and AST is Aspartate Transaminase

$P>0.05$ =Non significant and  $P<0.001$  highly significant (\*\*\*)

## DISCUSSION

Magnetic nanoparticles have been proposed for biomedical pur-

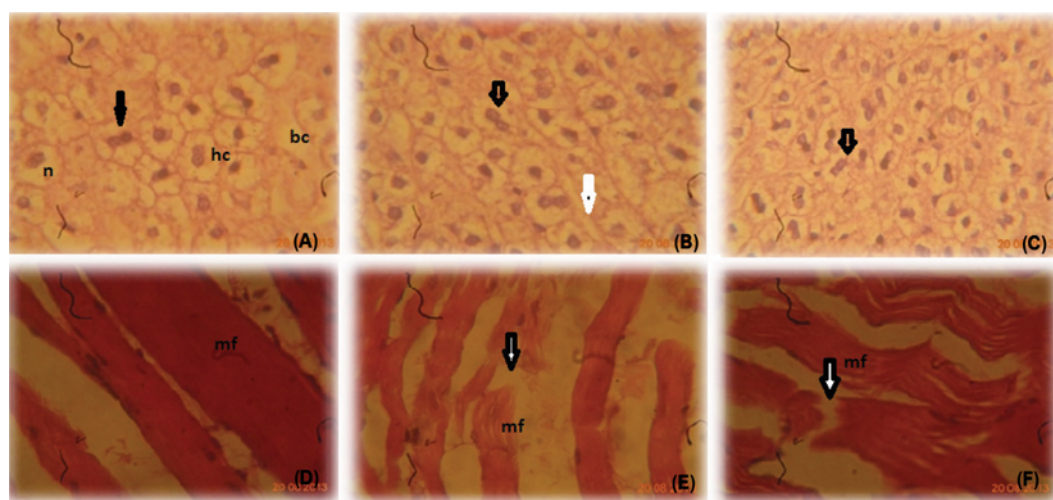


**Fig. 4.** Comparison of liver and muscle histology in adult male rabbits (*Lepus nigricollis*) between T1 (sham surgery) (A), (D), T2 (Intraperitoneal implantation of 1 mg/Kg body weight of  $\text{CoFe}_2\text{O}_4$ ) (B), (E) and T3 (Intraperitoneal implantation of 10 mg/Kg body weight  $\text{CoFe}_2\text{O}_4$ ) (C), (F). A is untreated liver slide showing healthy hepatocyte. Black arrowheads showing nuclear division (hc: Hepatocyte, bc: Bile canaliculi, n: Nucleus). (B) and (C), liver section exposed to  $\text{CoFe}_2\text{O}_4$  (B), (C) increased sinusoidal spaces (white bold arrow), (D) Normal muscle histology with compact myofibrils (mf). (E), (F) ruptured myofibrils (black arrows).



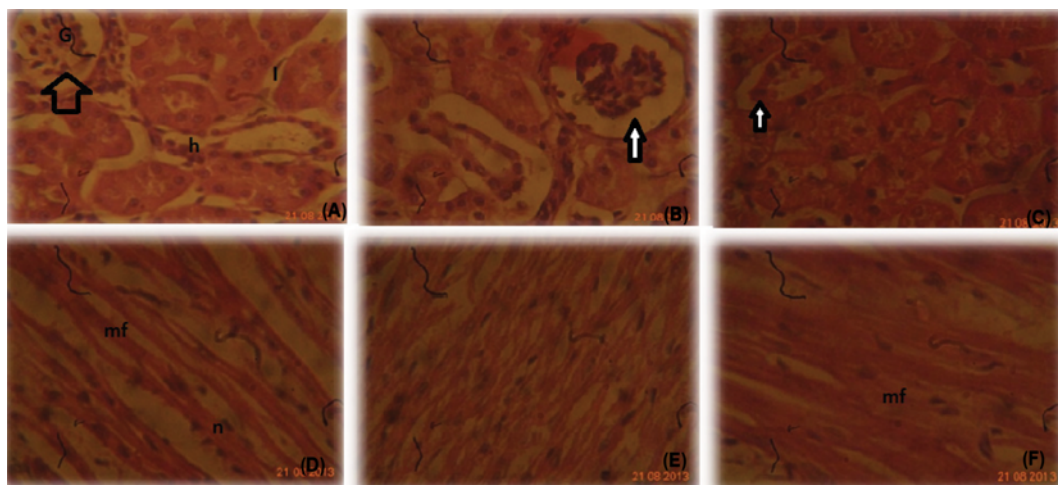


**Fig. 5.** Comparison of kidney and heart histology in adult male rabbits (*Lepus nigricollis*) between T1 (sham surgery) (A), (D), T2 (Intraperitoneal implantation of 1 mg/Kg body weight of  $\text{CoFe}_2\text{O}_4$ ) (B), (E) and T3 (Intraperitoneal implantation of 10 mg/Kg body weight  $\text{CoFe}_2\text{O}_4$ ) (C), (F). (A) Normal kidney histology (G, glomerulus, h: hematopoietic tissue, I: Interstitial Space in kidney Parenchyma). (B), (C) cellular infiltration (Bold arrow) and shrinkage of tuft of capillaries in glomerulus (White arrow), (D)-(F) normal cardiac muscle histology with compact muscle fibers (mf) and nucleus (n).

poses to a large extent for several years. In recent years, nanotechnology has developed to a stage that makes it possible to produce, characterize and specifically tailor the functional properties of nanoparticles for clinical applications [19]. This has led to various opportunities such as improving the quality of magnetic resonance imaging, hyperthermic treatment for malignant cells, site-specific drug delivery and the manipulation of cell membranes [20]. Mostly, these particles can easily penetrate the membranes of cells. As these are treated as extracellular materials, some of the particles hamper the normal functioning of the cell and sometimes they are fatal [21]. As little information is available regarding the biocompatibility of cobalt iron oxide, the present study was aimed to report the effect of a low and a high dose of these magnetic nanoparticles on blood chemistry and histology of vital organs in our experimental animal, the male rabbit.

It has been reported that the particles of smaller size have higher dissolution rate as compared to agglomerated (larger particles) in the gastric fluid, and the animals are more sensitive to smaller particles as compared larger ones [22]. Internalization of iron oxide particles strongly depends upon the size of the particles. After administration, larger particles with a diameter higher than 200 nm are easily sequestered by the spleen and eventually removed by the cells of the phagocyte system, resulting in decreased nanoparticle concentrations in the blood. Small particles with diameters less than 10 nm are rapidly removed through extravasations and renal clearance. Particles with a diameter ranging from 10 to 100 nm are optimal for intravenous injection and have the most prolonged blood circulation times. These particles are small enough to evade the RES of the body as well as to penetrate small capillaries of the tissues and offer the most effective distribution in targeted tissues [23]. In the present investigation, some of the particles agglomerate into larger particles, as indicated by the SEM image (Fig. 2). The non-agglomerated (smaller) particles play a major toxic role due to their higher dissolution. Our results indicated that the crystalline struc-

ture of nanoparticles was in 30 to 50 nm size range, and as per the results of Laurent et al. [23] these  $\text{CoFe}_2\text{O}_4$  nanoparticles can be effectively distributed to blood capillaries and to various tissues, supporting our results as we have reported drastic effect of intraperitoneal implantation of  $\text{CoFe}_2\text{O}_4$  on blood chemistry as well as on histology of vital organs.

A hematological analysis is routinely used in determining the physiological state of animals, which is known to be affected by different environmental factors and is used as a guide in the diagnosis of many diseases in both animals and humans [24]. Analysis of the results revealed a severe effect of  $\text{CoFe}_2\text{O}_4$  magnetic nanoparticles on complete blood count of rabbits in a dose-dependent manner (Table 1). We observed a severe decrease in WBC and lymphocyte count in T3 (exposed to high dose of  $\text{CoFe}_2\text{O}_4$ ), indicating that nanoparticles at high dose are affecting the WBC production and hence affecting the immune system of the animals (Table 1). Such low WBC can lead to various types of infection in body as white blood cells count gets so low to ward off bacteria and it also delays wound healing [25]. While in T2 we observed an extraordinarily high WBC, i.e., leukocytosis. WBC levels may increase due to increased marrow production or their decreased exit from the blood to the tissues [26]. An increase in the WBC count is a typical response to noxious stimuli and is usually part of an inflammatory reaction. A leukocytosis is frequently accompanied by cytologic abnormalities, such as toxic granulation or Dohle bodies [27].

Platelets play important role in homeostasis, minimize blood loss by contraction of damaged blood vessels and accelerate blood coagulation [28] and inflammatory processes [29]. In the present study, platelets were the most severely affected blood cells following  $\text{CoFe}_2\text{O}_4$  exposure, and a significant decrease was observed in both low and high dose treatments (Table 1), indicating that  $\text{CoFe}_2\text{O}_4$  exposure may lead to thrombocytopenia, which can lead to prolonged bleeding time, increased hemorrhaging and defective clot

formation [30].

Aspartate aminotransferase (AST) and alanine aminotransferase (ALT) are found in the liver, and due to diseases or injuries when the cells are destroyed, these enzymes are released into plasma and are considered as indicator of abnormal physiology [31]. We observed increased AST and ALT concentrations in cobalt iron oxide treatments, indicating a dose-dependent damage to liver function (Table 2). Several studies have reported similar observations in a variety of animals following exposure to toxicants, but limited comparative data is available regarding the effect of nanoparticle exposure on liver function. Hussain et al. [32] conducted in vitro studies in rat liver cell lines to demonstrate the toxicity of various nanoparticles at lower and higher dose concentrations, and they reported that  $\text{Fe}_3\text{O}_4$ , Al,  $\text{MoO}_3$  and  $\text{TiO}_2$  had no measurable effect at lower doses (10-50  $\mu\text{g}/\text{ml}$ ), while there was a significant effect at higher levels (100-250  $\mu\text{g}/\text{ml}$ ) especially on mitochondrial function and LDH leakage, indicating that the behavior of nanoparticles in the biosystem varies with their concentration.

Hussain et al. [32] demonstrated the toxicity of various nanoparticles in rat liver cells, in vitro, at lower and higher dose concentrations; their microscopic studies demonstrated that nanoparticle-exposed cells at higher doses became abnormal in size, displaying cellular shrinkage, and an acquisition of an irregular shape. We also observed a similar effect of in vivo  $\text{CoFe}_2\text{O}_4$  on the histology of vital organs and site of its implantation in male rabbits. The histology of liver and kidney was especially affected in both low and high dose treatments (Fig. 4, 5), indicating the toxic nature of this magnetic nanoparticles for a living system.

## CONCLUSION

Based on the hematological, serum biochemical and histological observations, we conclude that  $\text{CoFe}_2\text{O}_4$  nanoparticles cannot be recommended to be used in manufacturing the materials at both the concentrations applied in the present study, as it has drastic effects on the complete blood count, serum biochemical profile and on the histology of selected vital organs in adult male rabbits. We recommend further size-dependent studies with these nanoparticles that may lead to mechanism of action of  $\text{CoFe}_2\text{O}_4$  nanoparticles in living systems. Least toxic dose determination is also necessary so that these nano materials can be used in an effective and harmless manner.

## CONFLICT OF INTEREST

Authors have no conflict of interest of any sort with anyone.

## REFERENCES

1. L. B. Bangs, *Pure Appl. Chem.*, **68**, 1873 (1996).
2. P. D. Rye, *Biotechnol.*, **14**, 155 (1996).
3. C. Sangregorio, J. K. Wiemann, C. J. O. Connor and Z. Rosenzweig, *J. Appl. Phys.*, **85**, 5699 (1999).
4. H. Pardoe, W. Chua-Anusorn, T. G. St Pierre and J. Dobson, *J. Magn. Magn. Mater.*, **225**, 41 (2001).
5. A. Tibbe, B. de Grooth, J. Greve, P. Liberti, G. Dolan and L. Terstappen, *Nat. Biotechnol.*, **17**, 1210 (1999).
6. Y. Kularatne, P. Lorigan, S. Browne, S. K. Suvarna, M. Smith and J. Lawry, *Cytomet.*, **50**, 160 (2002).
7. R. E. Zigeuner, R. Riesenberger, H. Pohla, A. Hofstetter and R. Oberneder, *J. Urol.*, **169**, 701 (2003).
8. F. X. Cheng, Z. Y. Peng, C. S. Liao, Z. G. Xu, S. Gao, C. H. Yan, D. Wang and J. Wang, *Solid State Commun.*, **107**, 471 (1996).
9. Y. C. Mattei, O. P. Perez, M. S. Tomar, F. Roman, P. M. Voyles and W. G. Stratton, *J. Appl. Phys.*, **103**, 506 (2008).
10. A. F. Ju'nior, V. Zapf and P. Egan, *J. Appl. Phys.*, **101**, 500 (2007).
11. C. H. Yan, Z. G. Xu, F. X. Cheng, Z. M. Wang, L. D. Sun, C. S. Liao, et al., *Solid State Commun.*, **111**, 287 (1999).
12. S. Ammar, A. Helfen, N. Jouini, F. Fievet, I. Rosenman, F. Villain, P. Molinie and M. Danot, *J. Mater. Chem.*, **11**, 186 (2001).
13. N. Moumen, P. Veillet and M. P. Pileni, *J. Magn. Magn. Mater.*, **149**, 67 (1995).
14. C. N. Chinnasamy, B. Jeyadevan, O. Perales-Perez, K. Shinoda, K. Tohji and A. Kasuya, *IEEE. Trans. Magn.*, **38**, 2640 (2002).
15. M. Rajendran, R. C. Pullar, A. K. Bhattacharya, D. Das, S. N. Chintalapudi and S. K. J. *J. Magn. Magn. Mater.*, **232**, 71 (2001).
16. M. Grigorova, H. J. Blythe, V. Blaskov, V. Rusanov, V. Petkov, V. Masheva, D. Nihtianova, L. M. Martinez, J. S. Muñoz and M. Mikhov, *J. Magn. Magn. Mater.*, **183**, 163 (1998).
17. K. Laznev, D. Tzerkovsky, K. Kekalo, G. Zhavnerko and V. Agabekov, *IEEE. Trans. Magnet.*, **49**, 425 (2013).
18. P. M. Tamhankar, A. M. Kulkarni and S. C. Watawe, *Mater. Sci. Appl.*, **2**, 1317 (2011).
19. X. Liu, Y. Guan, Z. A. Ma and H. Liu, *Langmuir*, **20**, 10278 (2004).
20. A. K. Gupta and M. Gupta, *Biomater.*, **26**, 3995 (2005).
21. W. Voit, D. K. Kim, W. Zapka, M. Muhammed and K. V. Rao, *Mater. Res. Soc.*, **676**, 1 (2001).
22. B. Wang, W. Feng, M. Wang, T. Wang, Y. Gu, M. Zhu, H. Ouyang, J. Shi, F. Zhang, Y. Zhao, Z. Chai, H. Wang and J. Wang, *J. Nanopar. Res.*, **10**, 263 (2008).
23. S. Laurent, D. Forge, M. Port, A. Roch, C. Robic, L. V. Elst and R. L. Muller, *Chem. Rev.*, **108**, 2064 (2008).
24. S. G. Solomon and V. T. Okomoda, *J. Stress Physio. Biochem.*, **8**, 247 (2012).
25. G. K. Iwama, A. D. Pickering, J. P. Sumpter and C. B. Schreck, *Fish stress and health in aquaculture*, Cambridge University Press, England (2011).
26. D. L. Gardner and D. E. F. Tweedle, *Pathology for surgeons in training*, CRC Press, Boca Raton, Florida, USA (2002).
27. A. Bradran and H. Nasri, *J. Ayub Med. Coll. Abbottabad.*, **18**, 22 (2006).
28. Lippincott, *Anatomy and Physiology made incredibly visual*, Lippincott Williams and Wilkins, USA (2009).
29. P. T. K. Woo and D. W. Bruno, *Fish diseases and disorders: Viral, bacterial and fungal infections*, Oxfordshire, UK (2011).
30. L. S. Shapiro, *Pathology and parasitology for veterinary technicians*, Cengage learning, USA (2009).
31. D. D. Pratt and M. M. Kalpan, *N. Eng. Med. J.*, **342**, 1266 (2000).
32. S. M. Hussain, K. L. Hess, J. M. Gearhart, K. T. Geiss and J. J. Schlager, *Toxicol. In Vitro.*, **19**, 975 (2005).